UGC Approved Journal

IARJSET

ISSN (Online) 2393-8021
ISSN (Print) 2394-1588

International Advanced Research Journal in Science, Engineering and Technology

ISO 3297:2007 Certified

Vol. 4, Issue 7, July 2017

Sol-gel Auto Combustion Synthesis, Structural and Micro Structural Investigations on Cr^{3+} Doped $Y_3Fe_5O_{12}$ Garnet Nanoparticles

J. Y. Kadam[1], Ashok V. Humbe[2], Pankaj P. Khirade[2], Shankar D. Birajdar[2], R. G. Dorik[3], K. M. Jadhav[2]

Department of Physics, Balbhim Art's, Science & Commerce College, Beed, (MS) India[1]

Department of Physics, Dr. Babasaheb Ambedkar Marathwada University, Aurangabad, (MS) India[2]

Department of Physics, Vivekanand College, Aurangabad, (M.S.) India[3]

Abstract: The nanocrystalline yttrium iron garnet and chromium (Cr^{3+}) substituted yttrium iron garnet $Y_3Fe_{5-x}Cr_xO_{12}$ (x=0.00, 0.20 and 0.40) ceramics was prepared by citric acid assisted sol-gel auto combustion. The produced phases were characterized by X-ray diffraction (XRD). Particles of uniform size around 74–93 nm were obtained in the cubic structure of the prepared samples. Various structural parameters such as lattice constant (a), X-ray density (d_x), unit cell volume (V) etc. were calculated from the XRD data. The variation of these structural parameters in chromium composition has been studied. The lattice constant decreases while X-ray density increases with increasing Cr content x. The morphology revealed by scanning electron microscopy (SEM) images suggests the fluffy, porous and mud like structure. It is also observed that the grain of spherical shape with somewhat agglomerations. The agglomeration can be attributed to the magnetic interactions and high surface energy of prepared nanoparticles. FTIR spectra show typical absorption bands indicating the formation of garnet structure of the samples. Upon chromium substitution, absorption bands broadened and shifted towards lower wavenumber.

Keywords: Garnet, XRD, FTIR. sol-gel auto combustion.

I. INTRODUCTION

Yttrium iron garnet (YIG), is a microwave ferrite and has specific characteristics in polycrystalline form. Owing to its efficient handling of microwave power and with excellent magnetic and magneto-optical properties it has become a technologically significant material for making microwave frequency devices [1-3]. It is a soft ferrimagnetic material possessing cubic structure with Ia-3d space group. Its structure consists of three sub-lattices as the octahedral (a) site occupied by two iron ions, the dodecahedral (c) site occupied by three yttrium ions and the tetrahedral (d) site occupied by three iron ions. Both (Y^{3+} and Fe^{3+}) the trivalent metallic ions present in these sites make it an exceptionally suitable material for magnetic investigations. The most important interaction is the super-exchange interaction between iron ions at octahedral and tetrahedral sites. Due to its good characteristics in Faraday rotation it is being extensively used for the magneto-optical applications like optical isolators, magnetic sensors, circulators, phase shifter, etc. The substituted YIG have found their extensive use in non-reciprocal microwave devices. It is well known fact that the microstructure of sintered materials depends very much on the characteristics of the initial powders. There are ample of synthesis routes which can be employed for the synthesis of garnets such as co-precipitation [4, 5], sol-gel auto combustion [6, 7], solid state reaction technique[8], modified conventional mixed oxide[9], self combustion [10], etc.
Communication systems have created the need of materials having narrow resonant linewidth and low saturation magnetization. Yttrium iron garnets are the suitable for these demands because they possess the narrow resonant linewidth, low saturation magnetization, high electrical resistivity, high radiation and chemical stability, low thermal expansion, better electromagnetic properties, low loss, etc.

The polycrystalline YIG as a function of preparative parameters viz. sintering time, temperature etc were investigated by number of researchers [11-13]. Geller et. al. [14] reported magnetic behavior of heavier rare-earth garnets. The magnetic interactions in YIG which are related to the inter sub-lattice exchanges, that is super exchange interaction between Fe^{3+} iron in octahedral and tetrahedral sites through O^{2-} ions. These sub-lattices of YIG can be tailored by substituting various cations in a structure leading to changes in magnetic properties. The composition and homogeneity are the essential aspects of the garnets material preparation, as both strongly determine the its magnetic properties. Al^{3+} element is paramagnetic and has the preference towards, the tetrahedral sites. Thus, the substitution of Al^{3+} may lead to a substantial modification in magnetic and electrical properties of YIG.
The present work reports the synthesis of $Y_3Fe_{5-x}Cr_xO_{12}$ (x = 0.00, 0.20 and 0.40) by sol-gel auto combustion technique and experimental results obtained on the crystallographic and morphological properties of $Y_3Fe_{5-x}Cr_xO_{12}$.

UGC Approved Journal

IARJSET

ISSN (Online) 2393-8021
ISSN (Print) 2394-1588

International Advanced Research Journal in Science, Engineering and Technology

ISO 3297:2007 Certified

Vol. 4, Issue 7, July 2017

II. EXPERIMENTAL

Materials

Yttrium nitrate $Y_3(NO_3)_3.H_2O$, Iron nitrate $Fe(NO_3)_3.9H_2O$, Chromium nitrate $Cr(NO_3)_3.6H_2O$ and Citric acid $C_6H_8O_7.H_2O$.

Synthesis

The YIG and Cr substituted YIG nanoparticles of the chemical formula $Y_3Fe_{5-x}Cr_xO_{12}$ (x=0.00, 0.20 and 0.40) were prepared by sol-gel auto combustion synthesis route. The metal nitrates were used as oxidants while the citric acid was selected as fuel. Following raw materials purchased by Merck with purity 99.99% were used without further purification during the synthesis of the YIG and Cr substituted YIG samples.

The starting materials were weighed according to the chemical formula for each composition and dissolved in minimum amount of distilled water.

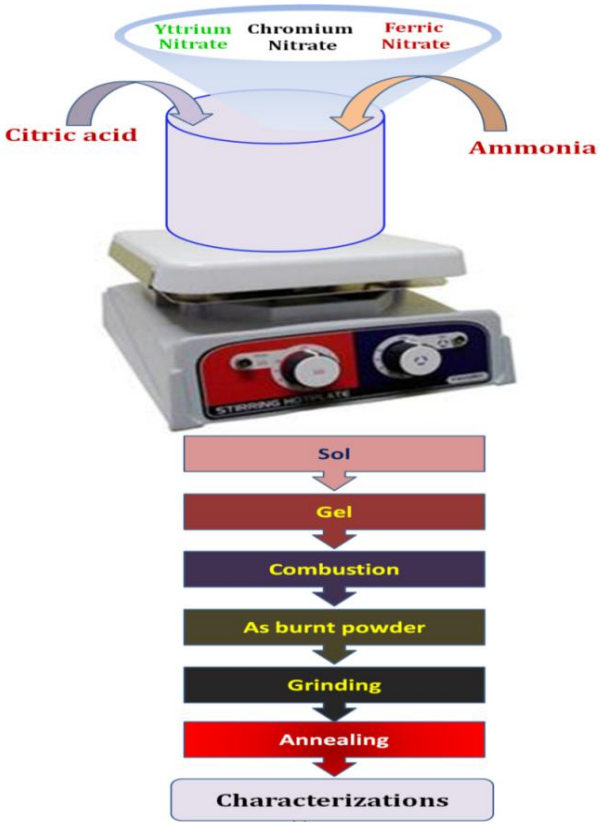

Fig. 1. Schematic flowchart of sol-gel auto combustion synthesis route for preparation of $Y_3Fe_{5-x}Cr_xO_{12}$

In particular, each metal nitrate and citric acid were dissolved in 100 ml distilled water and mixed together. The mixed solution of all nitrates was continuously stirred at 50^0C on magnetic stirrer with hot plate until a completely dissolved solution was obtained.

Then the solution of citric acid was added as a fuel to the mixed solution of metal nitrates and heated at 90^0C. Upon continuous heating, the sol converted to gel, very viscous gel and combustion took place and formed a powder. Various stages of the synthesis using sol-gel auto combustion are presented in the flowchart as shown in Fig. 1. The combusted powder was ground using agate pestle mortar. The obtained fine powder was annealed at 950^0C for 24 h. The annealed powder was used for the structural and morphological characterizations.

Characterizations

The structural characterizations of YIG and Cr substituted YIG nanoparticles were carried out by X-ray diffraction (XRD) of Rigaku in 2θ range of 20-80 degrees with Cu-Kα radiation at room temperature. The nature and phase purity of the prepared YIG and Al substituted YIG samples were checked by XRD patterns. Other structural parameters were also determined from XRD data. The morphology of $Y_3Fe_{2-x}Cr_xO_{12}$ (x=0.00, 0.20, 0.40) ceramics was carried out by scanning electron microscopy (SEM) (ZEISS EVO 18 special edition) technique Fourier transform infrared (FTIR) spectrometer was employed for the extraction of the characteristics bands of metal-oxygen environment in frequency range of 400-4000 cm^{-1}.

UGC Approved Journal

IARJSET

ISSN (Online) 2393-8021
ISSN (Print) 2394-1588

International Advanced Research Journal in Science, Engineering and Technology

ISO 3297:2007 Certified

Vol. 4, Issue 7, July 2017

III.RESULTS AND DISCUSSIONS

X-ray diffraction (XRD) patterns recorded at ambient temperature of $Y_3Fe_{5-x}Cr_xO_{12}$ (x=0.00, 0.20, 0.40) ceramics prepared by citric acid assisted sol-gel auto combustion technique are depicted in Fig. 2.

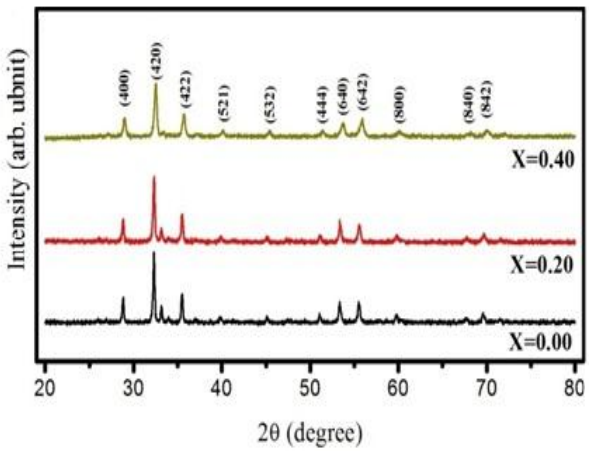

Fig. 2. XRD patterns of $Y_3Fe_{5-x}Cr_xO_{12}$ (x=0.00, 0.20 and 0.40)

From Fig. 2 it is revealed that the diffraction peaks relevant to garnet structure are present. The peaks (400), (420), (422), etc which belongs to garnet structure are sharply reflected. The observed XRD patterns of Cr substituted YIG samples revealed the presence of cubic phase structure along with secondary phase of $YFeO_3$. However, the intensity of the secondary phase peak decreases with Cr concentration increases.

Furthermore, the values of Miller indices (h k l), Bragg's angle (θ), interplanar spacing (d) and intensity (I) obtained from XRD data. The lattice parameter (a) values of YIG and Cr substituted YIG samples were calculated using standard relation,

$$a = d\sqrt{(h^2+k^2+l^2)} \quad Å \qquad \ldots 1$$

where, (d) is interplanar spacing and (h k l) is Miller Indices.
The obtained values of the lattice parameter (a) are tabulated in table 1. It was found that the lattice parameter decreases with increase in Cr concentration. The decrease in lattice parameter with Cr content 'x' is according to Vegard's law and can be interpreted on the basis of the smaller ionic radii of the constituent Cr ion [15]. In the present system larger Fe^{3+} ions are replaced by smaller Cr^{3+} ions. This decreases the d-spacing which leads to the decrease in lattice parameter. The variation of lattice parameter with chromium content 'x' is similar to that reported in the literature.

The unit cell volume (V) was calculated by using the following equation;

$$V = a^3 \quad Å \qquad \ldots 2$$

where, V is the unit cell volume and a is the lattice constant.
The unit cell volume (V) shows gradual decrease with the substitution of chromium. The decrease in unit cell volume is attributed to decrease in lattice parameter of the system under investigation.

The X-ray density (d_x) was calculated by using the relation and values are summarized in table 1;

$$d_x = \frac{Z \times M}{V \times N_A} \quad gm/cm^3 \qquad \ldots 3$$

where, Z is the number of molecules per formula unit, M is molecular mass of the sample, $V= a^3$ is the unit cell volume and N_A is the Avogadro's number.
It can be observed from table 1that X-ray density increases as Cr content x. The observed increase in X-ray density can be due to the increase in molecular weight / mass which overtakes the decrease in volume.
The bulk density of the present sample was obtained through Archimedes principle using toluene as an immersion liquid. The values of bulk density are reported in table 1. It is evident from table 1 that bulk density also decreases with Cr content x.
The crystallite size of the YIG and Cr substituted YIG was calculated by using the most intense peak (420) and using the Debye-Scherer's relation for small and uniform sized cubic crystals,

UGC Approved Journal

IARJSET

ISSN (Online) 2393-8021
ISSN (Print) 2394-1588

International Advanced Research Journal in Science, Engineering and Technology

ISO 3297:2007 Certified

Vol. 4, Issue 7, July 2017

$$t = \frac{0.9\lambda}{\beta \cos\theta} \quad \text{nm} \qquad \ldots 4$$

where, λ is wavelength of the Cu-Kα radiation, β is the full width of the half maximum, θ is Bragg's angle.
The obtained values of the crystallite size are presented in table 1. The average crystallite size calculated by using Debye Scherer's formula is varying from 74 - 93 nm.
The scanning electron microscopy (SEM) technique was employed for the analysis of the morphology. Fig. 3 shows the typical SEM image of x = 0.00 sample.

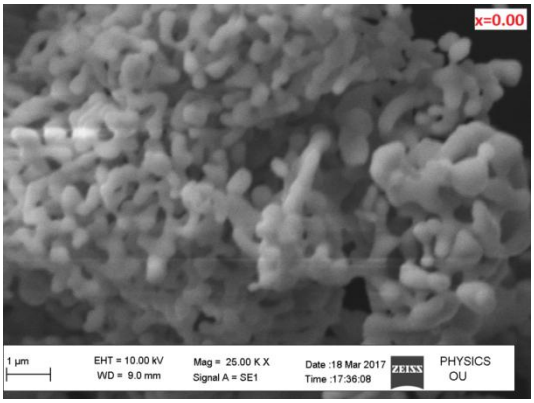

Fig. 3. Typical SEM image of $Y_3Fe_{5-x}Cr_xO_{12}$ (x=0.00)

The morphology revealed by SEM images suggests the fluffy, porous and mud like structure. It is also observed that the grain of spherical shape with somewhat agglomerations. The agglomeration can be attributed to the magnetic interactions and high surface energy of prepared nanoparticles. Furthermore, SEM images are composed of no regular shaped grains with elongated grains. The observed grain size varies in the range of 257 nm -383nm, such a large grain size be corresponds to the high annealing temperature (950^0C) which may lead to grain growth. Thus, large grain size was observed.
A comprehensive study of Fourier transform infrared spectra is essential to understand the garnet phase formation, which provides the necessary information regarding the structure, bond strength, imperfection and impurities. Fig. 4 shows FTIR spectra of Cr substituted YIG nanoparticles. The band positions determined from FTIR spectra for each samples are tabulated in table 2. In the infrared region, the molecular vibration gives rise to absorption bands, which identify the vibration modes associated with the tetrahedral metal-oxygen. The vibrational frequency depends upon the cation mass, cation oxygen bonding force, distance etc. FTIR spectrum for YIG (x=0.00) exhibits three bands at around 542cm^{-1} and 602cm^{-1} which can be assigned to the stretching mode of the tetrahedral site in the YIG structure. This observation indicates that the crystallization of YIG sample is completed. Similar results were obtained for YIG by other researchers [16]. The modes ranging from 860cm^{-1}-860cm^{-1} can be assigned to the stretching of C=O in carbonates. Moreover, the vibration bands ranging from 1645cm^{-1}-1649cm^{-1} can be associated to the deformation of O-H bonds which can be attributed to the adsorbed water molecules. Furthermore, the absorption peaks at 3437cm^{-1}, 3446cm^{-1} and 3436cm^{-1} are corresponding to the stretching vibrations of O-H due to absorption of water molecules. In case of Cr substitution, the absorption bands are found to slightly broadened and shifted towards higher wavenumber.

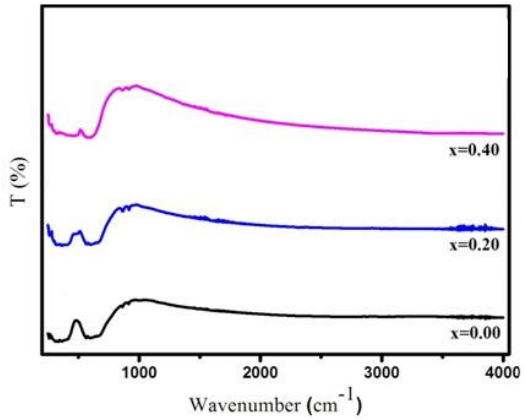

Fig. 4. FTIR spectra of $Y_3Fe_{5-x}Al_xO_{12}$ (x=0.00, 0.20, and 0.40)

UGC Approved Journal

IARJSET

ISSN (Online) 2393-8021
ISSN (Print) 2394-1588

International Advanced Research Journal in Science, Engineering and Technology

ISO 3297:2007 Certified

Vol. 4, Issue 7, July 2017

Table 1. Lattice parameter (a), Unit cell volume (V), X-ray density (d_x), Bulk density (d_B) and Crystallite size (t) of $Y_3Fe_{5-x}Cr_XO_{12}$ (x= 0.00, 0.20 and 0.40)

x	A (Å)	V ($Å^3$)	d_x (gm/cm^3)	d_B (gm/cm^3)	T (nm)
0.0	12.369	1892.3	4.978	3.682	93
0.2	12.356	1886.2	4.989	3.667	82
0.4	12.341	1879.7	4.990	3.627	74

Table 2. Vibrational bands of $Y_3Fe_{5-x}Cr_XO_{12}$ (x= 0.00, 0.20 and 0.40)

'x'	Vibrational absorption bands (cm^{-1})		
0.0	364	566	364
0.2	361	598	361
0. 4	360	600	360

IV. CONCLUSION

The nanocrystalline yttrium iron garnet and chromium substituted yttrium iron garnet $Y_3Fe_{5-x}Al_xO_{12}$ (x=0.00, 0.20, and 0.40) ceramics was prepared by citric acid assisted sol-gel auto combustion. The phase of garnet formation along with other secondary phases was observed from XRD patterns of the investigated samples. The lattice parameter decreased with Cr substitution due to its smaller ionic radius. X-ray density of YIG was found to decrease with Cr substitution. SEM images revealed fluffy, porous and mud like morphology with agglomeration of grains. The grain size is obtained to be in the nanometer range. FTIR spectra show typical absorption bands indicating the formation of garnet phase. Upon chromium substitution, absorption bands broadened and shifted towards lower wavenumber.

REFERENCES

[1] Shastry S, Srinivasan G, Bichurin M, Petrov V, Tatarenko A. Microwave magnetoelectric effects in single crystal bilayers of yttrium iron garnet and lead magnesium niobate-lead titanate. Physical Review B 2004;70:064416.
[2] Carter PS. Magnetically-tunable microwave filters using single-crystal yttrium-iron-garnet resonators. IRE Transactions on Microwave Theory and Techniques 1961;9:252-60.
[3] Tsai CS, Su J. A wideband electronically tunable microwave notch filter in yttrium iron garnet–gallium arsenide material structure. Applied physics letters 1999;74:2079-80.
[4] Jafelicci M, Godoi R. Preparation and characterization of spherical yttrium iron garnet via coprecipitation. Journal of magnetism and magnetic materials 2001;226:1421-3.
[5] Vaqueiro P, López-Quintela MA, Rivas J. Synthesis of yttrium iron garnet nanoparticlesvia coprecipitation in microemulsion. Journal of Materials Chemistry 1997;7:501-4.
[6] Shaiboub R, Ibrahim NBy, Abdullah M, Abdulhade F. The physical properties of erbium-doped yttrium iron garnet films prepared by sol-gel method. Journal of Nanomaterials 2012;2012:2.
[7] Vajargah SH, Hosseini HM, Nemati Z. Synthesis of nanocrystalline yttrium iron garnets by sol–gel combustion process: The influence of pH of precursor solution. Materials Science and Engineering: B 2006;129:211-5.
[8] Ali WFFW, Othman M, Ain MF, Abdullah NS, Ahmad ZA. Studies on the formation of yttrium iron garnet (YIG) through stoichiometry modification prepared by conventional solid-state method. Journal of the European Ceramic Society 2013;33:1317-24.
[9] Abbas Z, Al-Habashi RM, Khalid K, Moksin A, Maarof M. Garnet ferrite (Y3Fe5O12) nanoparticles prepared via modified conventional mixing oxides (MCMO) method. European Journal of Scientific Research 2009;36:154-60.
[10] Kuznetsov MV, Pankhurst QA, Parkin IP, Affleck L, Morozov YG. Self-propagating high temperature synthesis of yttrium iron chromium garnets Y3Fe5− xCrxO12 (0≤ x≤ 0.6). Journal of Materials Chemistry 2000;10:755-60.
[11] Sharma PU. Investigations on the effect of thermal history, particle size and SHI irradiation on some physical properties of Y3+-substituted YIG: Saurashtra University; 2009.
[12] Ganne J-P, Lebourgeois R, Paté M, Dubreuil D, Pinier L, Pascard H. The electromagnetic properties of Cu-substituted garnets with low sintering temperature. Journal of the European Ceramic Society 2007;27:2771-7.
[13] Panda S, Upadhyaya A, Agrawal D. Effect of conventional and microwave sintering on the properties of yttria alumina garnet-dispersed austenitic stainless steel. Metallurgical and materials transactions A 2006;37:2253-64.
[14] Geller S, Remeika J, Sherwood R, Williams H, Espinosa G. Magnetic study of the heavier rare-earth iron garnets. Physical Review 1965;137:A1034.
[15] Vithal Vinayak, Pankaj P. Khirade, Shankar D. Birajdar, R.C.Alange, K. M. Jadhav Electrical and Dielectrical Properties of Low-Temperature-Synthesized Nanocrystalline Mg2+-Substituted Cobalt Spinel Ferrite, J Supercond Nov Magn, (2015) 28:3351–3356
[16] Campbell AMHaKR. Infrared spectroscopy of yttrium aluminum, yttrium gallium, and yttrium iron garnets. Journal of Applied Physics 1992;72:638